Received: 6 August 2024 | Revised: 15 October 2024 | Accepted: 21 October 2024

DOI: 10.1002/joa3.13179

ORIGINAL ARTICLE

Journal of Arrhythmia Open Access WILEY

Achieving reduced radiation exposure with maintained fluoroscopy effectiveness using ultralow-dose settings in cryoballoon ablation

Takashi Kaneshiro M.D.[1] | Sadahiro Murota M.D.[1] | Takeshi Nehashi M.D.[1] | Minoru Nodera M.D.[1] | Shinya Yamada M.D.[1,2] | Masamitsu Ikeda R.T.[3] | Yasuchika Takeishi M.D.[1]

[1]Department of Cardiovascular Medicine, Fukushima Medical University, Fukushima, Japan

[2]Department of Arrhythmia and Cardiac Pacing, Fukushima Medical University, Fukushima, Japan

[3]Department of Radiology, Fukushima Medical University, Fukushima, Japan

Correspondence
Takashi Kaneshiro, Department of Cardiovascular Medicine, Fukushima Medical University, 1 Hikarigaoka, Fukushima 960-1295, Japan.
Email: tk2435@fmu.ac.jp

Abstract

Background and Aims: Optimization of fluoroscopic image quality for reducing radiation exposure in cryoballoon pulmonary vein isolation (CB-PVI) has not yet been fully investigated. Therefore, we tried to compare the radiation doses among three different X-ray system settings.

Methods: Consecutive 148 patients scheduled for their first CB-PVI were prospectively enrolled: low dose with the use of an anti-scatter grid for the first 51 patients (LD + G group), low dose without an anti-scatter grid for the subsequent 46 patients (LD-G group), and ultralow dose (ULD group) with an anti-scatter grid for the remaining 51 patients. We compared the radiation doses required to complete CB-PVI procedures among the groups. There were 27 patients for whom CB-PVI was performed without cine acquisition, but with fluoroscopy only, and the radiation doses were also compared.

Results: The median procedure time and fluoroscopy time were 119 and 35.5 min, respectively, with no significant differences among the groups. The median cumulative air Kerma (AK) decreased in both the LD-G group (71.8 mGy, $p < .001$) and the ULD group (73.0 mGy, $p < .001$), compared to the LD + G group (145.0 mGy). Among 27 patients who underwent CB-PVI without cine acquisition, the median cumulative AK further decreased in both the LD-G group (31.4 mGy, $p < .05$) and the ULD group (22.7 mGy, $p < .01$), compared to the LD + G group (64.6 mGy).

Conclusion: Using an ULD X-ray setting and avoiding cine acquisition, we can reduce radiation exposure, while ensuring the necessary fluoroscopy time for the CB-PVI procedure.

KEYWORDS
atrial fibrillation, cryoballoon pulmonary vein isolation, radiation exposure, ultralow-dose setting

1 | INTRODUCTION

Pulmonary vein (PV) isolation using cryoballoon (CB) has a considerable cooling effect, which can create durable lesions in the PV antrum and achieve better clinical outcomes in patients with paroxysmal and persistent atrial fibrillation.[1–4] Although pulmonary vein isolation (PVI) can be performed with less radiation exposure using radiofrequency ablation guided by a three-dimensional electroanatomic mapping system, the CB catheter cannot be integrated into such mapping system. Therefore, CB pulmonary vein isolation (CB-PVI) is performed under X-ray guidance with radiation exposure to both patients and medical professionals.[5,6]

Radiation exposure poses a greater risk to medical professionals, particularly operators of ablation procedures. While patients may undergo procedures involving radiation exposure only a few times throughout their lives, medical professionals perform such procedures on a daily basis, thus receiving more exposure through their work. The potential cancer risk associated with procedural radiation exposure is an occupational health risk for operators.[7,8] Among interventional cardiologists, for instance, tumors on the left side of the brain, which is known to be more exposed to the radiation than the right side, have been reported more frequently than those in the right brain.[7,8] Chronic occupational radiation exposure may also be associated with an increased incidence of cataract, a direct effect on the gonads and hypothalamic–pituitary–gonadal axis, atherosclerosis, early vascular aging, and neurocognitive impairment.[9–13] However, as reported previously, interventional cardiologists tend to underestimate the lifetime cancer risk.[14,15]

Several methods to reduce exposure associated with electrophysiological procedures have been investigated, such as removing the anti-scatter grid and reducing radiation exposure time.[16–18] However, methods to optimize the image quality in such low-dose setting have not been fully evaluated, even though the CB-PVI procedure does not require images with particularly high resolution. Since a certain length of fluoroscopy time is necessary for safe performance of the procedure, we hypothesized that it may be possible to achieve both radiation exposure reduction and securing the necessary fluoroscopy time by optimizing the X-ray system settings. In the present study, we performed CB-PVI with different X-ray system settings in order to determine the optimal settings that can achieve these two objectives.

2 | METHODS

2.1 | Study design

We prospectively enrolled consecutive 148 patients who were scheduled for their first CB-PVI for drug-refractory AF in our institution between July 2022 and November 2023. We performed CB-PVI with three different X-ray settings: low dose with an anti-scatter grid in the first 51 patients (LD+G group); low dose without an anti-scatter grid in the subsequent 46 patients (LD-G group); and ultralow dose with an anti-scatter grid in the remaining 51 patients (ULD group). The settings for the ULD group were chosen with the aim of further reducing radiation exposure while achieving sufficient image quality by using an anti-scatter grid. We then evaluated the parameters of CB-PVI procedures and compared the radiation doses needed for CB-PVI procedures among the groups.

In the study population, there were 27 patients for whom CB-PVI was performed without cine acquisition, but with fluoroscopy only. We retrospectively compared the radiation doses of these patients in the three groups.

The study protocol was approved by the Research Ethics Committee of Fukushima Medical University, and written informed consent was obtained from all the patients prior to undergoing the procedure.

2.2 | Cryoballoon pulmonary vein isolation for atrial fibrillation

Catheter ablation was performed for AF following the cessation of all antiarrhythmic drugs for over five half-lives before the procedure. Preprocedural electrocardiogram-gated computed tomography was performed in all the patients, and the anatomy of the left atrium (LA) and PV in each patient was assessed. CB-PVI was performed using a CB catheter from either of two manufacturers (Arctic Fron Advance, Medtronic, Inc., Minneapolis, MN, or POLARx/POLARx FIT, Boston Scientific, Marlborough, MA) depending on the operator's preference. Immediately after vascular access was obtained, 3000 IU heparin was administered. The periprocedural activated clotting time was maintained at 300–400 s with a bolus infusion of 5000 IU heparin and a continuous infusion of heparin at a rate of 2000–3000 IU/h after a transseptal approach. A single transseptal puncture was performed using an 8.5 Fr long sheath (SL8.5, Abbott, Abbott Park, IL) and a radiofrequency needle (Japan Lifeline Co., Ltd., Tokyo, Japan). Two SL8.5 sheaths were inserted into the LA via the same puncture site and changed to a 15-Fr steerable sheath (Flexcath Advance, Medtronic, or POLARSHEATH, Boston Scientific). An eight-polar spiral mapping catheter (Achieve, Medtronic, or POLARMAP, Boston Scientific) was used for PV mapping. A CB catheter was advanced to each PV ostium over the spiral mapping catheter, and complete occlusion of the ostium was confirmed with an injection of 50% diluted contrast medium. The freezing time in one CB application was 3 min, and an additional CB was not applied after isolation was achieved. Because of a higher arrhythmogenicity in LSPV, freezing time of CB application for LSPV could be prolonged to 210–240 s at the operator's discretion. If the PV had not been completely occluded, CB ablation was performed multiple times at the upper and lower portions of the PV ostium. If the PV was not isolated with several CB ablations, additional touch-up radiofrequency catheter ablation was applied using a 7.5-Fr irrigation catheter with a 3.5-mm distal electrode and real-time contact force monitoring (ThermoCool ContactForce SF, Biosense Webster, Inc., Diamond Bar, CA). The endpoint of PVI was defined as the creation of a bidirectional conduction block between the LA and PVs. For patient safety, CB ablation was terminated when the balloon temperature fell below −60°C (Arctic Fron Advance, Medtronic) or below −70°C (POLARx/POLARx FIT, Boston Scientific).[2,19] We then monitored the diaphragmatic compound motor action potential during phrenic nerve pacing to avoid phrenic nerve injury, especially during CB ablations for the right PVs.

2.3 | X-ray system settings

All procedures were performed using an Azurion 7 B12 system (Philips N.V., Amsterdam, Netherlands), in two C-arm angulations: anteroposterior oblique or right anterior oblique 30° and left anterior oblique 60° with the heart being centered in both projections. The frame rate was set at 3.75 pulse/s and 15 frame/s during fluoroscopy and cine acquisition, respectively, in all patients. In both the LD+G and LD-G groups, the detector dose rate was set at 64 nGy/s during fluoroscopy and 60 nGy/frame during cine acquisition, and spectral beam filters containing 0.4 mm copper and 1.0 mm aluminum were used. The only difference between the two groups was whether or not an anti-scatter grid was used. In the ULD group, the detector dose rate was changed to 40 nGy/s during fluoroscopy and 40 nGy/frame during cine acquisition, and copper spectral beam filter was changed to 0.9 mm, and an anti-scatter grid was used. PV occlusion was confirmed with contrast medium injection and recorded by cine acquisition or fluoroscopy at the operator's discretion.

2.4 | Evaluation of procedural radiation exposure

For all procedures, the number of cine acquisition series, fluoroscopy time (min), cumulative dose area product (DAP; Gy·cm^2), and cumulative air Kerma (AK; mGy) values were documented. The DAP is defined as the absorbed dose multiplied by the irradiated area and it correlates with stochastic radiation effects. The AK represents the absorbed dose and correlates with deterministic radiation effects. DAP and AK for each patient were calculated separately for cine acquisitions and fluoroscopic images. We quantified the subjective evaluation of image quality by scoring with a 10-point scale (0: bad to 10: excellent) across the X-ray system settings. These parameters were calculated by averaging the values evaluated by three investigators, who were blinded to the X-ray system setting in each study subject.

2.5 | Statistical analyses

Normality of continuous variables was confirmed using a Shapiro–Wilk test. Normally distributed variables are presented as mean ± standard deviation, nonnormally distributed variables are presented as median (25th percentile–75th percentile), and categorical variables are expressed as counts and percentages. Normally and nonnormally distributed variables were compared using one-way ANOVA and a Kruskal–Wallis test, respectively. Then, the Bonferroni post hoc test was used to test the significant differences between the groups. A chi-squared test was used for the comparison of categorical variables. A two-sided p-value of <.05 was considered statistically significant. These analyses were performed using a statistical software package (SPSS ver. 21.0, IBM, Armonk, NY).

3 | RESULTS

3.1 | Baseline patient characteristics and procedural details

The clinical characteristics of the patients are summarized in Table 1. The mean age was 68.3 ± 8.5 years, and 49 of the 148 patients (33%) were female. Approximately 75% of the patients presented with paroxysmal AF. The mean LA diameter (LAD) and the median LA volume index (LAVI) in echocardiography were 40.5 ± 6.1 mm and 39.0 (32.8–50.0) mL/m^2, respectively.

The procedural details of CB-PVI are shown in Table 2. The PVs in all patients were successfully isolated. The median total number of freezing cycles and total freezing time in each PV were similar in all three groups. The median procedure time was 119 (97–149) min, with no significant differences among the groups. Fifty-six patients (38%) underwent the following additional procedures: cavo-tricuspid isthmus ablation in 47 patients, superior vena cava isolation in two patients, touch-up ablation of any PV in three patients, accessory pathway ablation in six patients, slow pathway ablation in two patients, and ablation for focal atrial tachycardia in one patient. No patient experienced any complications as a result of the CB-PVI procedure.

3.2 | Procedural parameters of radiation exposure

A detailed comparison of exposure doses among the three groups is shown in Table 3. The median number of cine acquisition series and fluoroscopy time were 6 (2–11) and 35.5 (29.3–45.9) min, respectively, and did not differ among the groups. The median cumulative DAP was lower in both the LD-G group (9.5 [6.3–13.6] Gy·cm^2, $p < .001$) and the ULD group (10.5 [4.4–17.0] Gy·cm^2, $p < .001$), compared to the LD+G group (18.1 [11.6–30.0] Gy·cm^2). The median cumulative AK was also lower in both the LD-G group (71.8 [40.6–106.8] mGy, $p < .001$) and the ULD group (73.0 [31.8–124.0] mGy, $p < .001$), compared to the LD+G group (145.0 [89.5–266.8] mGy). Although the same level of radiation dose reduction was achieved in both the LD-G and ULD groups, the quality of fluoroscopic images was improved in the ULD group compared to the LD-G group (Figure 1 and Video 1). As the results of quantifying the subjective evaluation of image quality, each median values of image quality scores were 7.0 (6.8–7.2) in the LD+G group, 5.8 (5.5–6.0) in the LD-G group, and 6.8 (6.5–7.0) in the ULD group (Table 3). There was no significant difference between the LD+G and ULD groups ($p = 0.067$) (Figure 2).

There were 27 patients in whom CB-PVI was performed without cine acquisition, but with fluoroscopy only (seven each in the LD+G and ULD groups and 13 in the LD-G group). Although the

TABLE 1 Baseline characteristics of patients in the three groups.

	Total ($n=148$)	LD + G ($n=51$)	LD-G ($n=46$)	ULD ($n=51$)	p-value
Age (years)	68.0 (61.0–74.0)	68.0 (60.5–73.0)	68.0 (62.3–74.0)	69.0 (61.0–74.0)	.563
Female (%)	49 (33%)	18 (35%)	17 (37%)	14 (27%)	.564
Persistent AF (%)	34 (23%)	14 (27%)	6 (13%)	14 (27%)	.158
Height (cm)	165 (157–170)	165 (156–169)	166 (158–170)	166 (156–172)	.746
Weight (kg)	64.2 (54.4–71.6)	64.9 (53.5–73.2)	61.4 (55.7–68.4)	64.4 (55.4–73.7)	.396
Body mass index (kg/m^2)	23.5 (21.5–25.9)	23.9 (22.1–26.1)	22.7 (20.9–24.6)	23.7 (21.5–26.0)	.195
LAD (mm)	40.5 ± 6.1	41.3 ± 7.3	40.0 ± 5.6	40.0 ± 5.2	.464
LAVI (mL/m^2)	39.0 (32.8–50.0)	40.0 (32.5–51.0)	39.5 (32.0–52.8)	38.0 (33.5–44.0)	.465

Note: Data are shown as the mean ± standard deviation, median (25th percentile–75th percentile), or number of patients (%).

Abbreviations: AF, atrial fibrillation; LAD, left atrial diameter; LAVI, left atrial volume index.

TABLE 2 Procedural parameters of cryoballoon pulmonary vein isolation among the three groups.

		Total ($n=148$)	LD + G ($n=51$)	LD–G ($n=46$)	ULD ($n=51$)	p-value
LSPV	Freezing cycles (number)	1.0 (1.0–1.0)	1.0 (1.0–1.0)	1.0 (1.0–1.0)	1.0 (1.0–1.0)	.716
	Freezing time (s)	200 (180–240)	180 (180–240)	180 (180–240)	210 (180–240)	.326
LIPV	Freezing cycles (number)	1.0 (1.0–1.0)	1.0 (1.0–1.0)	1.0 (1.0–1.0)	1.0 (1.0–1.0)	.481
	Freezing time (s)	180 (180–180)	180 (180–180)	180 (180–180)	180 (180–180)	.952
RSPV	Freezing cycles (number)	1.0 (1.0–2.0)	1.0 (1.0–2.0)	1.0 (1.0–2.0)	1.0 (1.0–2.0)	.736
	Freezing time (s)	180 (180–287)	180 (180–274)	180 (180–254)	180 (180–334)	.729
RIPV	Freezing cycles (number)	1.0 (1.0–2.0)	1.0 (1.0–2.0)	1.0 (1.0–2.0)	1.0 (1.0–1.8)	.949
	Freezing time (s)	180 (180–241)	180 (180–224)	180 (180–253)	180 (180–230)	.891
Procedure time (min)		119 (97–149)	120 (101–153)	118 (94–165)	116 (99–143)	.777
Additional procedure (%)		56 (38%)	22 (43%)	23 (50%)	11 (22%)*	.010

Note: Data are shown as the median (25th percentile–75th percentile) or number of patients (%).

Abbreviations: LAVI, left atrial volume index; LIPV, left inferior pulmonary vein; LSPV, left superior pulmonary vein; RIPV, right inferior pulmonary vein; RSPV, right superior pulmonary vein.

*Statistically significant against LD-G ($p<.05$).

TABLE 3 Procedural radiation exposure during cryoballoon pulmonary vein isolation among the three groups.

	Total ($n=148$)	LD + G ($n=51$)	LD–G ($n=46$)	ULD ($n=51$)	p-value
Cine acquisition series (number)	6 (2–11)	6 (3–11)	5 (0–8)	7 (2–12)	.096
Fluoroscopy time (min)	35.5 (29.3–45.9)	35.7 (28.4–44.5)	33.8 (28.6–48.6)	35.7 (30.3–44.0)	.990
Cumulative DAP (Gy·cm^2)	11.7 (7.0–20.1)	18.1 (11.6–30.0)	9.5 (6.3–13.6)***	10.5 (4.4–17.0)***	<.001
Cine acquisition DAP (Gy·cm^2)	2.4 (0.6–7.3)	4.7 (1.2–13.7)	1.4 (0–4.7)**	2.3 (0.3–6.3)	.002
Fluoroscopic DAP (Gy·cm^2)	8.8 (5.5–12.8)	11.4 (8.7–17.7)	6.5 (4.5–9.9)***	6.5 (4.2–10.7)***	<.001
Cumulative air Kerma (mGy)	90.1 (50.2–150.0)	145.0 (89.5–266.8)	71.8 (40.6–106.8)***	73.0 (31.8–124.0)***	<.001
Cine acquisition air Kerma (mGy)	18.4 (4.5–54.7)	41.9 (10.8–124.4)	12.6 (0–32.9)**	17.1 (2.4–46.4)*	.001
Fluoroscopic air Kerma (mGy)	64.9 (36.2–96.4)	90.1 (65.5–135.4)	49.7 (31.6–73.8)***	42.6 (25.5–75.3)***	<.001
Image quality score	6.7 (6.0–7.0)	7.0 (6.8–7.2)	5.8 (5.5–6.0)***	6.8 (6.5–7.0)	<.001

Note: Data are shown as median (25th percentile–75th percentile) or number of patients (%). Statistically significant against LD + G; *$p<.05$, **$p<.01$, ***$p<.001$.

Abbreviation: DAP, dose area product.

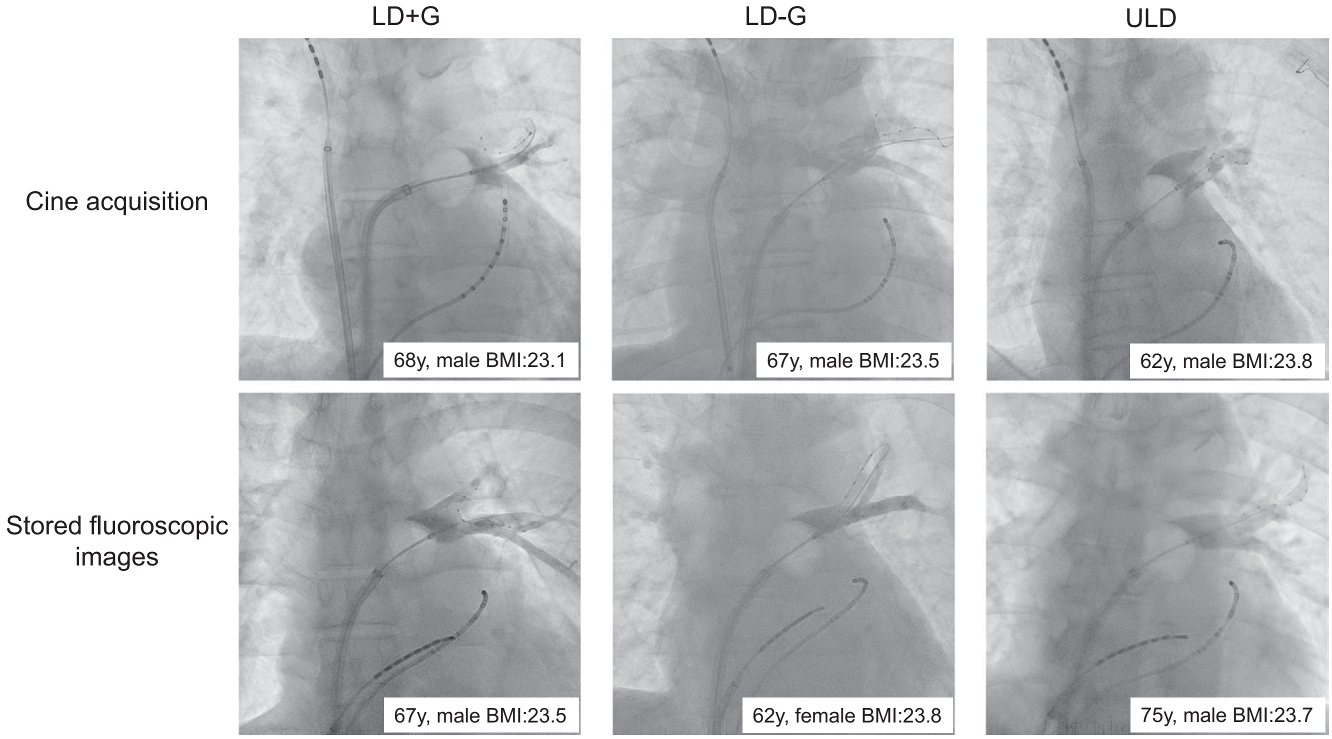

FIGURE 1 Comparison of cine acquisition and fluoroscopic images of representative patients from the three groups having similar body mass indexes. The upper row shows the cine acquisition image of a representative case of each group. The lower row shows the stored fluoroscopic image of a representative case of each group. Although the same level of radiation dose reduction was achieved in both the LD-G and ULD groups, the quality of fluoroscopic images was improved in the ULD group compared to the LD-G group. BMI, body mass index; LD+G, low dose with anti-scatter grid; LD-G, low dose without anti-scatter grid; ULD, ultralow dose.

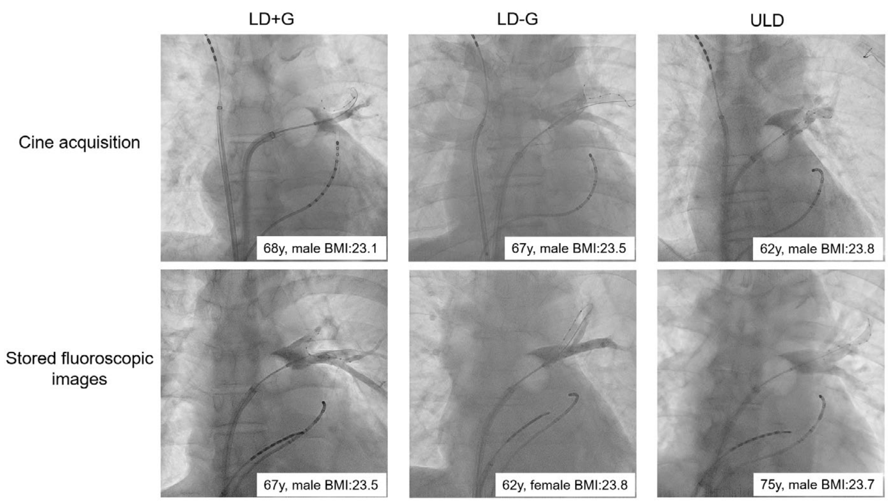

VIDEO 1 Comparison of cine acquisition and fluoroscopic images of representative patients from the three groups having similar body mass indexes. The upper row shows the cine acquisition video of a representative case of each group. The lower row shows the stored fluoroscopic image of a representative case of each group. Although the same level of radiation dose reduction was achieved in both the LD-G and ULD groups, the quality of fluoroscopic images was improved in the ULD group compared with the LD-G group. BMI, body mass index; LD+G, low dose with anti-scatter grid; LD-G, low dose without anti-scatter grid; ULD, ultralow dose. Video content can be viewed at https://onlinelibrary.wiley.com/doi/10.1002/joa3.13179

fluoroscopy time did not differ among the three groups (mean fluoroscopy time: 31.1 ± 8.3 min), the mean cumulative DAP was much lower in both the LD-G group (5.5 ± 2.5 Gy·cm^2, $p < .05$) and the ULD group (3.8 ± 1.0 Gy·cm^2, $p < .01$), compared to the LD+G group (8.8 ± 3.2 Gy·cm^2). The median cumulative AK was also lower in both the LD-G group (31.4 [25.5–46.1] mGy, $p < .05$) and the ULD group (22.7 [21.0–32.3] mGy, $p < .01$), compared to the LD+G group [64.6 (58.9–82.7) mGy]. These results strongly suggest that not performing cine acquisition during the CB-PVI procedure contributes to the significant reduction of radiation exposure (Table 4).

4 | DISCUSSION

The major finding of this study was that radiation exposure during CB-PVI can be reduced by optimizing the X-ray system settings, such as decreasing detector dose rates and using a thicker spectral beam filter. In addition, avoiding cine acquisition can further reduce radiation exposure while maintaining the quality of fluoroscopic images and ensuring necessary fluoroscopy time.

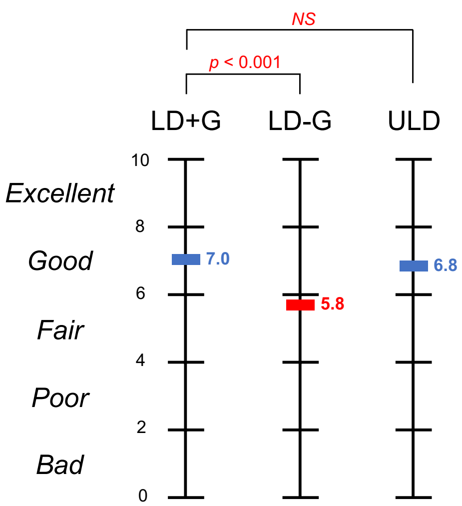

FIGURE 2 Results of quantifying the subjective evaluation of image quality. The median value of image quality score in the LD-G group was decreased compared to that in the LD+G group. However, there was no significant difference between the LD+G and ULD groups.

4.1 | Radiation exposure associated with CB-PVI procedure

Although PVI can be performed with less radiation exposure using radiofrequency ablation guided by a three-dimensional electroanatomic mapping system, CB cannot be integrated into such a mapping system. Therefore, the CB-PVI procedure should be performed under X-ray guidance, and radiation exposure to both patients and medical professionals is unavoidable.[5,6] Radiation exposure can be reduced by shortening fluoroscopy time, but a certain duration of fluoroscopy is required for safe performance of CB-PVI.

High-resolution fluoroscopic images are not necessary for electrophysiological procedures because the main purpose of fluoroscopy is to visualize relatively large objects, such as electrode and balloon catheters, sheaths, and the cardiac silhouette. Therefore, if these objects can be visualized clearly in X-ray images, it would contribute to both the reduction of radiation exposure and the securing of sufficient fluoroscopy time to perform the necessary procedure.

4.2 | Measures to reduce radiation exposure associated with CB-PVI procedure

4.2.1 | Use of a lower detector dose and a thicker spectral beam filter

Theoretically, radiation exposure can be reduced to zero by reducing the fluoroscopy time and a recently developed protocol aiming to minimize fluoroscopy time has been reported to significantly reduce radiation exposure.[18] However, as described above, we believe that it is desirable to retain a certain length of fluoroscopy time for safe and smooth performance of CB-PVI. A protocol

TABLE 4 Basic characteristics of and procedural parameters for 27 patients without cine acquisition.

	Total ($n=27$)	LD+G ($n=7$)	LD–G ($n=13$)	ULD ($n=7$)	p-value
Age (years)	68.3 ± 8.5	68.3 ± 7.9	67.5 ± 9.3	69.7 ± 8.6	.862
Female (%)	12 (44%)	4 (57%)	6 (46%)	3 (43%)	.855
Persistent AF (%)	1 (4%)	1 (14%)	0 (0%)	0 (0%)	.240
Hight (cm)	162 ± 9	158 ± 8	162 ± 8	165 ± 11	.348
Weight (kg)	59.5 ± 10.2	57.8 ± 11.4	59.6 ± 10.5	61.0 ± 9.8	.851
Body mass index (kg/m^2)	22.1 (21.2–24.3)	23.1 (21.2–24.0)	22.0 (21.6–24.2)	22.1 (21.3–24.2)	.966
LAD (mm)	39.1 ± 5.5	39.4 ± 4.9	40.0 ± 5.9	37.0 ± 5.5	.514
LAVI (mL/m^2)	39.5 ± 10.1	39.0 ± 12.0	41.7 ± 10.8	35.9 ± 6.3	.481
Procedure time (min)	116.7 ± 32.0	119.7 ± 24.0	120.2 ± 40.8	107.3 ± 19.5	.678
Additional procedure (%)	9 (33%)	3 (43%)	6 (46%)	0 (0%)	.102
Fluoroscopy times (min)	31.1 ± 8.3	34.4 ± 10.1	29.9 ± 8.4	29.7 ± 6.3	.479
Fluoroscopic DAP (Gy·cm^2)	5.9 ± 3.0	8.9 ± 3.2	5.5 ± 2.5*	3.8 ± 1.0**	.002
Fluoroscopic air Kerma (mGy)	32.2 (24.5–58.9)	64.6 (58.9–82.7)	31.4 (25.5–46.1)*	22.7 (21.0–32.3)**	.004

Note: Data are shown as the mean ± standard deviation, median (25th percentile–75th percentile), or number of patients (%). Statistically significant against LD + G; *$p<.05$, **$p<.01$.

Abbreviations: AF, atrial fibrillation; DAP, dose area product; LAD, left atrial diameter; LAVI, left atrial volume index.

without using the anti-scatter grid has also been reported to reduce radiation exposure during catheter ablations.[16,17] The anti-scatter grid is used to improve contrast by removing scattered X-rays.[20] While removing the anti-scatter grid can reduce radiation exposure, it can also lead to deterioration of image quality. To solve these conflicting issues, we reduced the detector dose rate while using an anti-scatter grid to both reduce radiation exposure and maintain image quality.

Another method to reduce radiation exposure is to use a thicker spectral beam filter. In the present study, we used a 0.4 mm copper filter and a 1.0 mm aluminum filter for the LD + G and LD-G groups while a 0.9 mm copper filter and a 1.0 mm aluminum filter for the ULD group. Using a copper-containing spectral beam filter has been shown to reduce radiation exposure during fluoroscopy without deterioration of image quality.[21,22] In the present study, radiation exposure (especially the patient dose) was further reduced by thickening the copper spectral beam filter. The combination of an ultra-low detector dose and a thicker copper spectral beam filter was found to be the optimal setting, which reduced radiation exposure by 70% according to our theoretical calculation.

4.2.2 | Avoiding cine acquisition

The analysis of patients who underwent CB-PVI without cine acquisition but with fluoroscopy only suggests that avoiding cine acquisition significantly contributed to reducing radiation exposure. In general, dose rates used in cine mode are about 10-fold higher than those in fluoroscopic mode. For the CB-PVI procedure, storing fluoroscopic images is sufficient for recording PV occlusion, eliminating the need for cine acquisition.

4.3 | Image quality necessary for the CB-PVI procedure

The intentionally decreased image quality of cine/fluoroscopy may compromise the safe and smooth performance of CB-PVI. However, both the procedure time and the fluoroscopy time did not differ among the three groups in the present study, and these parameters were similar to those of the previous studies.[4–6] Moreover, quantifying the subjective evaluation of image quality revealed no significant difference in image quality between the LD + G and the ULD groups. No patient experienced any complication associated with this procedure, showing the safety of this method.

4.4 | Clinical implications

Optimizing X-ray system settings, including the use of a lowered detector dose, an anti-scatter grid, and a thicker spectral beam filter, and avoiding cine acquisition during CB-PVI contribute not only to reducing radiation exposure on the side of patients but also to preventing occupational health risks of medical professionals involved in treatment.[7–15] This method can be adopted without any cost and could be adapted to other cardiovascular interventions that do not require high-resolution fluoroscopic images, such as device implantation, right heart catheterization, and cardiac biopsy.

4.5 | Study limitations

There are two limitations to the present study. First, the fluoroscopy time in the present study is the sum of single-plane and biplane fluoroscopy because the X-ray system can provide the total fluoroscopy time, but not the breakdown for each phase. Second, the fluoroscopic image quality cannot be quantitatively evaluated. Therefore, quantitative analysis of the images obtained should be considered in future studies.

5 | CONCLUSIONS

By optimizing X-ray system settings and avoiding cine acquisitions, reduction of radiation exposure and ensuring the necessary fluoroscopy time could be achieved even while keeping the quality of fluoroscopic images. For instance, a fluoroscopy time of approximately 30 min can yield X-ray images of reasonable quality and radiation exposure of less than 30 mGy.

AUTHOR CONTRIBUTIONS

Takashi Kaneshiro: Concept/design, data analysis/interpretation, drafting the article, statistics, and data collection. **Sadahiro Murota, Takeshi Nehashi, Minoru Nodera, Shinya Yamada, and Masamitsu Ikeda:** Approval of the article and data collection. **Yasuchika Takeishi:** Critical revision and approval of the article.

ACKNOWLEDGMENTS

The authors wish to thank Mr. Yuya Hasegawa (Phillips Japan) for his advice on the optimization of the X-ray system settings.

CONFLICT OF INTEREST STATEMENT

Shinya Yamada belongs to the Department of Arrhythmia and Cardiac Pacing, which is supported by Abbott Medical Japan Co., Ltd., Biotronik Japan Inc., and Nihon Kohden Corp. These companies are not associated with the contents of this study.

DATA AVAILABILITY STATEMENT

The data that support the findings of this study are available from the corresponding author upon reasonable request.

ETHICS STATEMENT

The study protocol was approved by the Ethics Committee of Fukushima Medical University.

PATIENT CONSENT STATEMENT

Written informed consent was obtained from all study subjects.

ORCID

Takashi Kaneshiro https://orcid.org/0000-0002-5284-9538
Shinya Yamada https://orcid.org/0000-0001-5726-3926

REFERENCES

1. Ciconte G, de Asmundis C, Sieira J, Conte G, Di Giovanni G, Mugnai G, et al. Single 3-minute freeze for second-generation cryoballoon ablation: one-year follow-up after pulmonary vein isolation. Heart Rhythm. 2015;12:673–80.
2. Su W, Kowal R, Kowalski M, Metzner A, Svinarich JT, Wheelan K, et al. Best practice guide for cryoballoon ablation in atrial fibrillation: the complication experience of more than 3000 procedures. Heart Rhythm. 2015;12:1658–66.
3. Wazni OM, Dandamudi G, Sood N, Hoyt R, Tyler J, Durrani S, et al. STOP AF first trial investigators. Cryoballoon ablation as initial therapy for atrial fibrillation. N Engl J Med. 2021;384:316–24.
4. Su WW, Reddy VY, Bhasin K, Champagne J, Sangrigoli RM, Braegelmann KM, et al. STOP persistent AF investigators. Cryoballoon ablation of pulmonary veins for persistent atrial fibrillation: results from the multicenter STOP persistent AF trial. Heart Rhythm. 2020;17:1841–7.
5. Andrade JG, Champagne J, Dubuc M, Deyell MW, Verma A, Macle L, et al. Cryoballoon or radiofrequency ablation for atrial fibrillation assessed by continuous monitoring. Circulation. 2019;140:1779–88.
6. Sørensen SK, Johannessen A, Worck R, Hansen ML, Hansen J. Radiofrequency versus cryoballoon catheter ablation for paroxysmal atrial fibrillation: durability of pulmonary vein isolation and effect on atrial fibrillation burden: the RACE-AF randomized controlled trial. Circ Arrhythm Electrophysiol. 2021;14:e009573.
7. Roguin A, Goldstein J, Bar O. Brain tumors among interventional cardiologists: a cause for alarm? Report of four new cases from two cities and a review of the literature. Euro Intervention. 2012;7:1081–6.
8. Filkelstein MM. Is brain cancer an occupational disease of cardiologists? Can J Cardiol. 1998;14:1385–8.
9. Little MP, Kitahara CM, Cahoon EK, Bernier MO, Velazquez-Kronen R, Doody MM, et al. Occupational radiation exposure and risk of cataract incidence in a cohort of US radiologic technologists. Eur J Epidemiol. 2018;33:1179–91.
10. Elmaraezy A, Ebraheem Morra M, Tarek Mohammed A, Al-Habaa A, Elgebaly A, Abdelmotaleb Ghazy A, et al. Risk of cataract among interventional cardiologists and catheterization lab staff: a systematic review and meta-analysis. Catheter Cardiovasc Interv. 2017;90:1–9.
11. Sarkozy A, De Potter T, Heidbuchel H, Ernst S, Kosiuk J, Vano E, et al. Occupational radiation exposure in the electrophysiology laboratory with a focus on personnel with reproductive potential and during pregnancy: a European heart rhythm association (EHRA) consensus document endorsed by the Heart Rhythm Society (HRS). Europace. 2017;19:1909–22.
12. Andreassi MG, Piccaluga E, Gargani L, Sabatino L, Borghini A, Faita F, et al. Subclinical carotid atherosclerosis and early vascular aging from chronic low-dose ionizing radiation exposure: a genetic, telomere and vascular ultrasound study in cardiac catheterization laboratory staff. JACC Cardiovasc Interv. 2015;8:616–27.
13. Borghini A, Vecoli C, Mercuri A, Carpeggiani C, Piccaluga E, Guagliumi G, et al. Low-dose exposure to ionizing radiation deregulates the brain-specific miR-134 in interventional cardiologists. Circulation. 2017;136:2516–8.
14. Giaccardi M, Anselmino M, Del Greco M, Mascia G, Paoletti Perini A, Mascia P, et al. Radiation awareness in an Italian multispecialist sample assessed with a web-based survey. Acta Cardiol. 2021;76:307–11.
15. Einstein AJ, Tilkemeier P, Fazel R, Rakotoarivelo H, Shaw LJ, American Society of Nuclear Cardiology. Radiation safety in nuclear cardiology—current knowledge and practice: results from the 2011 American Society of Nuclear Cardiology member survey. JAMA Intern Med. 2013;173:1021–3.
16. Smith IR, Stafford WJ, Hayes JR, Adsett MC, Dauber KM, Rivers JT. Radiation risk reduction in cardiac electrophysiology through use of a gridless imaging technique. Europace. 2016;18:121–30.
17. Attanasio P, Schreiber T, Pieske B, Blaschke F, Boldt LH, Haverkamp W, et al. Pushing the limits: establishing an ultra-low framerate and antiscatter grid-less radiation protocol for left atrial ablations. Europace. 2018;20:604–7.
18. Muñoz DR, Del Castillo AM, Al-Mahdi EAR, Rivera CL, Cienfuegos MG, Jiménez JR, et al. Systematic workflow and electrogram guidance to reduce X-ray exposure time during cryoballoon ablation of atrial fibrillation: the SWEET-Cryo strategy. Europace. 2023;25:euad231. https://doi.org/10.1093/europace/euad231
19. Heeger CH, Pott A, Sohns C, Riesinger L, Sommer P, Gasperetti A, et al. Novel cryoballoon ablation system for pulmonary vein isolation: multicenter assessment of efficacy and safety-Antarctica study. Europace. 2022;24:1917–25.
20. Barmes GT. Contrast and scatter in X-ray imaging. Radiographics. 1991;11:307–23.
21. Eichenlaub M, Astheimer K, Minners J, Blum T, Restle C, Maring C, et al. Evaluation of a new ultralow-dose radiation protocol for electrophysiological device implantation: a near-zero fluoroscopy approach for device implantation. Heart Rhythm. 2020;17:90–7.
22. Davies AG, Gislason-Lee AJ, Cowen AR, Kengyelics SM, Lupton M, Moore J, et al. Does the use of additional X-ray beam filtration during cine acquisition reduce clinical image quality and effective dose in cardiac interventional imaging? Radiat Prot Dosim. 2014;162:597–604.

How to cite this article: Kaneshiro T, Murota S, Nehashi T, Nodera M, Yamada S, Ikeda M, et al. Achieving reduced radiation exposure with maintained fluoroscopy effectiveness using ultralow-dose settings in cryoballoon ablation. J Arrhythmia. 2024;40:1400–1407. https://doi.org/10.1002/joa3.13179